Development and application of normalized spectral index based on hyperspectral imagery classification

Zhang Dongyan[1,2], Zhao Jinling[1,2], Huang Linsheng[1,2], Ma Wenqiu[2]

(1. Key Laboratory of Intelligent Computing & Signal Processing, Ministry of Education, Hefei 230039, China;
2. Beijing Research Center for Information Technology in Agriculture, Beijing 100097, China)

Abstract: Near-ground imaging spectroscopy applied in field provides new opportunity for development of quantitative remote sensing in agriculture. It deserves concern about how to exert its data advantage of integrating image and spectra into one, particularly in analyzing the influence of background targets, such as soil, shadow on crop nutrient inversion model. In this research, imaging cubes of wheat group in the field were collected by visible/near-infrared imaging spectrometer (VNIS). A normalized spectral index was set up according to reflectance characteristics of illuminated soil, shadow soil, illuminated leaf and shadow leaf in the image. Furthermore, the index was used to extract spectra of different targets in soybean images and analyze the variation of determination coefficient R^2 between normalized spectra of soybean group and chlorophyll density before and after removing background soil. The results showed that when spectra of soil and shadow leaf were removed, the sensitive bands of chlorophyll density shifted from red and near-infrared ranges (727 nm, 922 nm) to red ranges (710 nm, 711 nm), meanwhile, the overall trend was that visible ranges increased, near-infrared regions decreased and red bands had the highest determination coefficient. Therefore, it can be concluded that spectral purification based on normalized spectral index has important significance for quantitative research in agricultural remote sensing.

Key words: hyperspectral imaging; normalized spectral index; imagery classification; spectrum purification; wheat; soybean

CLC number: S127 **Document code:** A **Article ID:** 1007-2276(2014)02-0586-09

用于高光谱图像分类的归一化光谱指数的构建与应用

张东彦[1,2],赵晋陵[1,2],黄林生[1,2],马雯萩[2]

(1. 安徽大学 智能计算与信号处理教育部重点实验室,安徽 合肥 230039;
2. 北京农业信息技术研究中心,北京 100097)

摘 要: 成像高光谱的近地田间应用为农业定量遥感的发展提供了新的契机。如何发挥其图谱合一的数据优势,尤其在解析土壤、阴影等背景地物对作物养分反演模型的影响需要关注。该研究借助可见/近红外

收稿日期:2013-06-20; **修订日期**:2013-07-25

基金项目:国家自然科学基金(41301471); 教育部博士点基金项目(20133401120003);安徽大学青年科学研究基金(KJQN1121);安徽大学研究生学术创新研究项目(YQH100165);安徽省高等学校省级自然科学研究项目(KJ2013A026);安徽省自然科学基金(1308085QC58);中国博士后科学基金(2013T60189, 2012M520445);安徽大学博士科研启动项目

作者简介:张东彦(1982-),男,讲师,博士,主要从事高光谱遥感与图像处理方面的研究。Email:zhangdy@nercita.org.cn

通讯作者:黄林生(1977-),男,讲师,博士,主要从事高光谱遥感应用研究。Email:linsheng0808@163.com

成像高光仪,在近地田间采集小麦群体的成像立方体,根据影像中光照裸土、阴影裸土、光照叶片和阴影叶片的反射光谱特征建立了归一化光谱分类指数,并应用该指数提取大豆影像中不同类型地物的光谱,分析了背景土壤剔除前后的大豆植被归一化光谱与叶绿素密度的决定系数变化情况。结果表明:土壤和阴影叶片光谱去除后,反演叶绿素密度的敏感波段由红-近红外区间(727 nm, 922 nm)向蓝、绿,尤其是红波段(710 nm, 711 nm)移动。对叶绿素密度敏感的波段区间表现为可见光增加,近红外减少,且红边波段决定系数最高。由此说明,基于归一化光谱指数的植被光谱提纯对定量遥感反演研究具有重要意义。

关键词: 高光谱成像; 归一化光谱指数; 图像分类; 光谱提纯; 小麦; 大豆

0 Introduction

Presently, most classification methods for large-scale remote sensing image are proposed according to those images from satellite and aviation platforms. Since the spatial resolution (a pixel size) of their sensors is above meter-level, it is mainly used to distinguish crop or vegetation from target objects including residential area, bare soil, water body, road, etc. References[1-4] used classified satellite images including Landsat TM, Hyperion, SPOT, Quickbird and IKONOS to research land coverage change, forest biochemistry parameter mapping, rare tree extraction from grassland and urban vegetation drawing, etc. References[5-6] utilized classified aviation images including PHI and AVIRIS to research mapping of wheat biochemistry parameters and vegetation coverage extraction. The above classification methods of remote sensing images mainly are influenced by many kinds of targets, so classification accuracy of images is not high. The classification of small-scale image has spatial resolution of centimeter-level are conducted upon digital photo, those methods are mainly used for segmentation of crops or vegetation in the field from background targets, such as bare soil, weeds, crop straw, etc. Some researchers classified images of corn, wheat, soybean and rice, respectively[7-10], then explored change of crop coverage, segmented pest and disease damage area of crop leaf and constructed inversion models of crop biophysiological and biochemical parameters by using color characteristics [11-12]. The above proposed segmentation methods were mainly influenced by soil, weeds and crop residues. The main reason is that the scope of above image is limited; the target objects in the image are simple, mainly containing vegetation and soil, and red, green and blue bands. In recent years, near-ground imaging hyperspectral spectrometer with cm-level or mm-level spatial resolution has focused on agricultural quantitative remote sensing, and the report about classification methods of this sensor is rare. According to some scholars[13-14], spectral information of soybean and corn leaves was collected by imaging spectral system and quantitative inversion research was conducted for biochemistry parameters; pest and disease damage area of leaf was segmented by its spectra and image characteristic were researched[15-16]. The above researches were all restricted to mixed spectra of target objects. Still there was little research to analyze for inversion of crop physiological and biochemical parameters after classifying different targets from spectral images of field crop. Although researches were conducted by imaging sensor for wheat nitrogen in different nitrogen levels, spectral information used in modeling was still the mixed information of vegetation and background target without extensively exploring for the advantage of spectral information of pure vegetation[17-18]. Then, for this kind of spectral image, how to achieve division of different targets. Whether the inversion model of crop chlorophyll built with spectral information of pure vegetation after classification was better than the result of mixed vegetation. In view of this point, a

normalized spectral classification index was set up in this research according to reflectance characteristic of pure wheat vegetation, soil, sun leaf and shadow leaf in the image to achieve classification of targets after imaging cubes of field wheat group are collected by visible/near-infrared imaging spectrometer (VNIS). On this basis, this index was used to collect targets spectra in soybean image; then analyzed the variation of determination coefficient R^2 between normalized spectra of soybean group and chlorophyll density before and after removing background soil and evaluated its feasibility in near-ground imaging spectral classification. Finally it showed that vegetation spectral purification research was meaning for setup of quantitative remote sensing inversion model.

1 Materials and methods

1.1 Experimental design

Test 1: The soybean variety, zhonghuang13 was chosen as experimental material, and was seeded on July 1, 2010 with normal filed management. When soybean was flowering period, the field data was collected in State Precision Agriculture Research Demonstration Base in Xiaotangshan Town, Changping District, Beijing (40.18°N, 116.27°E) on August 29, 2010.

Test 2: Field calibration was conducted between ASD (ASD Field spec FR2500) and VNIS (visible and near-infrared imaging spectrometer) in Beijing Academy of Agriculture and Forestry Sciences (39.93° N, 116.27°E) on March 25, 2011. Blue cloth, green cloth, grey cloth, black cloth, standard white panel and standard grey panel were selected as standard reference objects and every data collection was completed in 30 minutes. During the period that standardization data was received, imaging data of wheat group during jointing stage was collected by VNIS.

It was sunny with gentle breeze when two tests were conducted; the time was from 10:00 am to 16:00 pm.

1.2 Instruments introduction

The instruments used in this research were VNIS and ASD. The sketch map was shown in Fig.1. The former is composed by a Hamamatsu C8484-05G camera, a V10E spectrograph, a 1.9/35 mm C-mount zoom lens, and a mirror scanner (Fig.1). The Hamamatsu C8484-05G is a high spectral resolution digital camera. The V10E spectrograph has a slit size of 30 μm by 14.3 mm and can collect hyperspectral imagery in the wavelength range of 400-1 000 nm with a spectral resolution of 2.8 nm. Together with the mirror scanner, the Hamamatsu C8484-05G collects the images in a push-broom manner and generates hyperspectral image cubes with effective pixels of 1 344 (spatial axis) by 1 024 (spectral axis). The angular field of view of the imaging spectrometer is 14° (horizontal) by 11° (vertical) by 18° (diagonal). The latter has 350-2 500 nm of spectral regions and 25° view field, in which its spectral resolution is 3 nm from 350 nm to 1 000 nm and spectrum sampling interval is 1.4 nm, but its spectral resolution is 10 nm and spectrum sampling interval is 2 nm from 1 000 nm to 2 500 nm. In this paper, wavelength of the ASD was interpolated to sampling interval of VNIS.

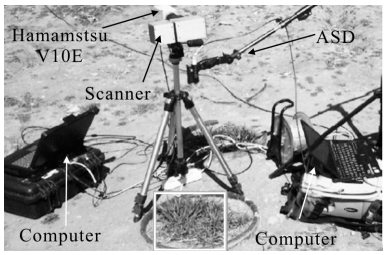

Fig.1 Demonstration of VNIS and ASD collecting data

1.3 Data collection and processing

When field calibration of VNIS was conducted with ASD, the observation height was fixed according to view range of two instruments. VNIS was placed on spider, 80 cm from mirror face to observation target. ASD was fixed on multi-purpose spider, 55 cm from the detector to observation target. Then, the view range of the former was a 25×25 cm^2 and the latter

was a circle with the diameter of 24.2 cm, which guaranteed visual range conformity of two instruments. When data collection was conducted for wheat canopy, the time difference of two instruments was 15 s and this guaranteed data were synchronously.

When imaging cube of soybean was collected by VNIS, the mirror face on the instrument was 178 cm to soybean canopy, and the view field was a 36×36 cm^2. The obtained hyperspectral images were transferred into relative reflectance and then applied in quantitative inversion research of corp. The relative reflectance inversion in this paper was referenced[19].

After spectral data was gathered, corresponding fresh plants were taken to measure chlorophyll density and the detailed measurement methods referenced[20].

2 Results

2.1 Development of normalized spectral index

2.1.1 Reduce the shadow effects

At present, spectral information of target object obtained either by imaging sensor or non-imaging sensor is mixed. In the field, this mixed information is jointly composed by crops, weeds, straw, soil and shadows. Studies have shown that, when growth monitoring and nutrient diagnosis were conducted by sensor for green vegetation, the shadows caused by different parts of the same target or different targets have certain influence on quantitative remote sensing diagnosis [21]. However, this problem is well resolved by imaging spectra. Fig.2 (a) was wheat spectral image under natural illumination. It was seen clearly that, left part area was obviously shadow region, which was caused by sheltering of leaves in the upper layer and it was hard to visually judge whether it was wheat leaf or soil. Then the result may have great error if different targets were classified directly by reflectance image. Normalized reflectance method (Formula 1) was used in this research to remove spectral difference between illuminated and shadow targets so that visual interpretation was resolved and imaging classification precision was improved [22-24]. Fig.2 (b) was the result of wheat reflectance image after normalized treatment. Comparing Figs.2(a) and 2(b), it was found that shadow leaf and shadow soil in the image were clearly showed to provide data support for threshold division of targets when image was classified.

$$R_{ij}=\frac{R_{ij}}{\left(\frac{1}{K}\sum_{j}R_{ij}\right)} \tag{1}$$

Where R_{ij} represents normalized reflectance, i, j represent starting and ending bands respectively and K represents the total number of bands.

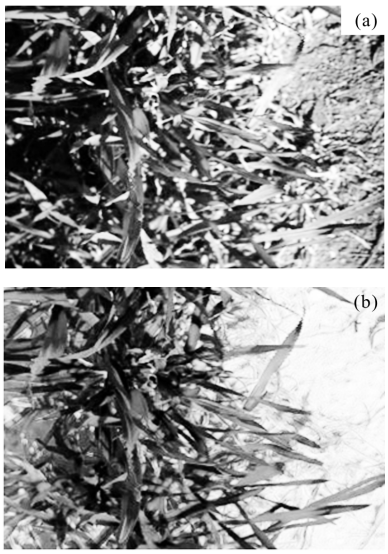

Fig.2 Original image and normalized spectral image

2.1.2 Normalized spectral index

Normalized spectral index proposed in this paper was calculated by selecting spectral characteristic value of different targets in the image within visible and near-infrared spectral bands. Spectral image involved in the research was mainly composed by illuminated leaf, sun soil, shadow leaf and shadow soil and their spectral reflectance curves were shown in Fig.3. Those four targets had obvious spectral characteristic difference at 551 nm (green peak), 670 nm (red valley) and 760-950 nm (near-infrared platform), meaning that green vegetation had obvious reflection peak at green peak in visible light bands; red valley had

obvious absorption feature and near-infrared band has high reflectance platform and the soil does neither reflection peak nor has absorption valley. For four targets, sun soil has the highest reflectance value at 670 nm and shadow leaf has the lowest reflectance value; the whole order was represented as sun soil > shadow soil > illuminated leaf > shadow leaf. However, at near-infrared platform, the reflectance value of shadow leaf was the highest and that of sun soil was the lowest, just opposite to the order at 670 nm, so the spectral feature at the two wavelengths could be used to distinguish four targets. It was also known from the Fig.3 that, four targets had obvious reflectance difference at the band of 551 nm, which could well distinguish soil from green vegetation, so this band was also chosen as featured wavelength. Based on above wavebands, normalized spectral index was built upon. Firstly, subtraction calculation was conducted by using 550 nm minus 670 nm. It must be in this order so that the index of sun soil and part shadow soil is negative, which can well separate soil from other targets. Secondly, that using 765 nm minus 670 nm, the threshold of shadow leaf can be highlighted to the greatest extend, which was convenient for shadow leaf division. Additionally, in order to get the maximum difference value in distinguishing different target types, after calculating the above wavebands, we can divide with spectral value at 670 nm so that division threshold values among different targets appear obvious value gradient. The formula (2) was the result of threshold division. The proposed normalized spectral index was shown in formula (3).

$$R_{\text{cal}}=\begin{cases} X<0;\ \text{Sun soil} \\ 0\leqslant X<0.12;\ \text{Shadow soil} \\ 0.12\leqslant X<3.0;\ \text{Sun leaf} \\ 3.0\leqslant X;\ \text{Shadow leaf} \end{cases} \tag{2}$$

$$R_{\text{cal}}=\frac{(R_1-R_2)}{R_2}\times(R_3-R_2) \tag{3}$$

Where R_1, R_2 and R_3 represent single wavelength of 551 nm, 670 nm and 765 nm respectively and R_{cal} represents result of bands calculation.

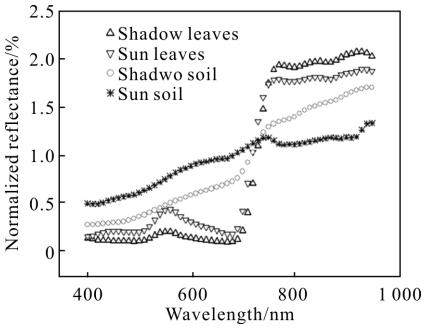

Fig.3 Spectral curves of different objects

2.1.3 Imagery classification and spectral purification

Based on the above band math, identified result of imagery classification was shown in Fig.4. The white part in the image represented sun soil; the brown part represented shadow soil; the light green part represented sun leaves and the dark green part represented shadow leaves. On this basis, mask treatment of image was conducted according to threshold regions among different targets. Figure 5 was

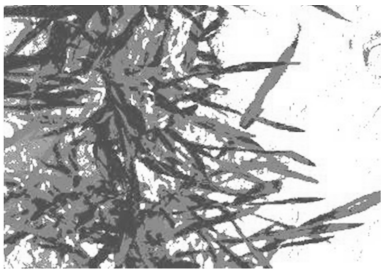

Fig.4 Identified result of imagery classification

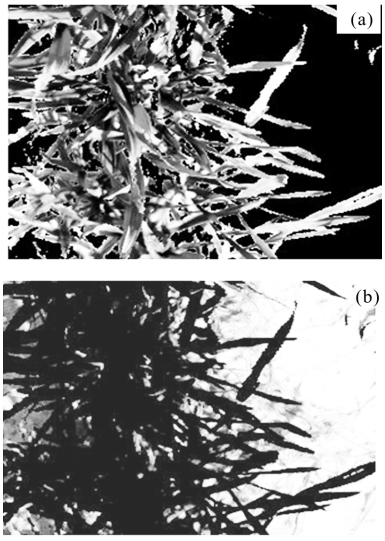

Fig.5 Masking images of wheat leaves and bare soil

the result map of wheat and soil after mask treatment. Among that, the black part in Fig.5 (a) represented sun soil and shadow soil and others represented wheat; the black part in Fig.5 (b) represented sun leaves and shadow leaves and others represented soil. By comparing Fig.5 (a) and Fig.5 (b), it was found good separation between wheat group and soil. In addition, spectral mean values of sun soil, shadow soil, sun leaves and shadow leaves were also extracted and the result was shown in Fig.6. Since the masked result was similar to Fig.5, the corresponding images in the paper were not listed.

The follow-up work of this research was to purify spectral information of different targets after imagery classification and the result was shown in Fig.6. It can be seen from the figure that reflectance spectra of mixed targets in visible and near-infrared bands was bigger than purified that, which was explained that background soil made great contribution to spectral enlargement; after background soil was masked, spectra of wheat leaves was rapidly decreased, especially showing in near-infrared band; shadow leaves of wheat was continued to be masked, reflectance of sun leaves continually decreased at near-infrared regions and was not obvious at visible light bands; and reflectance value of shadow leaves was the lowest at visible and near-infrared band. By analyzing the above results, it was known that background so il exerted great influence on spectral information obtained by sensor, especially at near-infrared band. Because multi-scattering phenomenon influenced light radiative transfer when background targets and target vegetation all existed, reflectivity at near-infrared band was obviously enlarged; meanwhile, shadow proportion of target was also a factor to impact on sensor to obtain spectral information. For example, reflectance of shadow leaves in Fig.6 had no obvious green peak characteristic at 551 nm and was almost a straight line from 400 nm to 700 nm, then shadow area directly influenced on spectral information quantity obtained from the researched target; finally impacted on analysis result of quantitative remote sensing. So, it had realistic significance to research for the influence of background target and shadow on the accuracy for diagnostic model of crop nutrient.

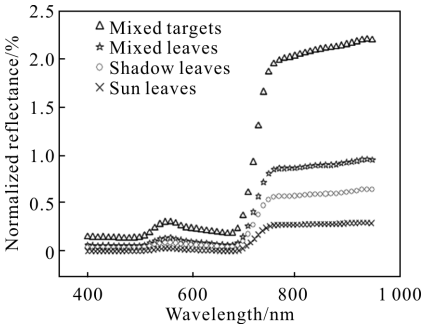

Fig.6 Spectral curves of different typological objects

2.2 Application of normalized spectral index

This research applied normalized spectral index to take spectral information of pure soybean vegetation, soil, sun leaves and shadow leaves from soybean images, respectively. The result was consistent with that in Fig.5, so it was not listed. Spectral influence of those components on crop chlorophyll density inversion was analyzed one by one and the significance of image classification on setup of crop quantitative remote sensing inversion model was discussed. Figures 7 (a), 7 (b) and 7 (c) were determination coefficients (R^2) between chlorophyll density and NDVI of mixed vegetation, pure vegetation, and illuminated vegetation.

It can be seen from Fig.7(a), when vegetation and soil existed as a mixed target, sensitive bands of chlorophyll were 727 nm and 922 nm, which came from red light and near infrared light, respectively, and it was consistence with construction principle of vegetation index NDVI. It meant that both were achieved based on combined operation of red and near infrared bands[25]. After soil spectra removed, sensitive bands became 710 nm and 711 nm, which all located at red light region, but sensitivity of blue and green light was obviously increased and it was consistence with principle proposed by predecessors that vegetation growth vigor was monitored by normalized difference

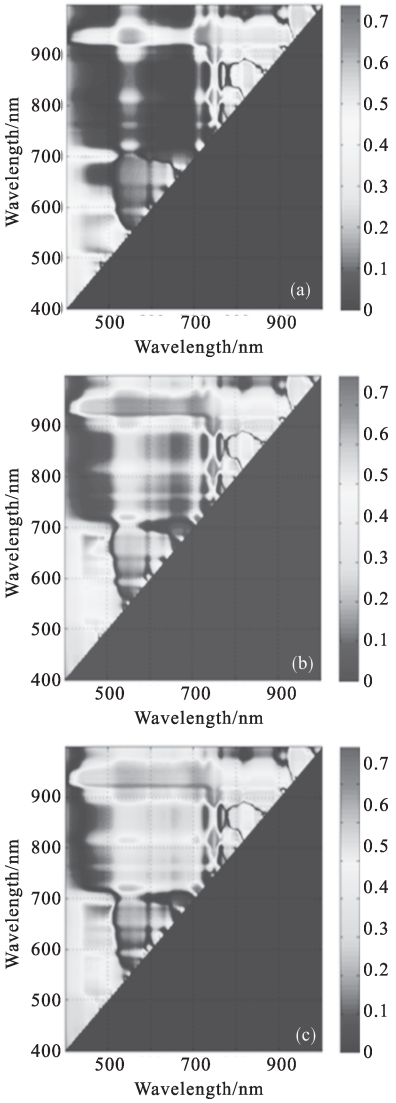

Fig.7 Determination coefficients (R^2) between chlorophyll density and NDVI of mixed vegetation(7(a)), pure vegetation(7(b)), illuminated vegetation(7(c))

green index and normalized difference vegetation index of blue and green bands [26-27]. Its determination coefficient with chlorophyll density was shown in Fig.7 (b), which showed that sensitive regions to chlorophyll density enlarged, especially in blue and green bands. It can be explained that background soil exerted great influence on monitoring biochemistry index of vegetation group using optics remote sensing and it was same to previous research results[28]. Based on this, in this paper, vegetation spectral information of shadow leaves was removed to attempt to analyze the influence extent of shadow part on quantitative remote sensing inversion and the result was shown in Fig.7(c). By comparing figures 7(c) and 7(b), it can be found that, after spectra of shadow leaves removed, sensitive bands to chlorophyll density were visible bands increased, near-infrared bands decreased and red bands had the highest determination coefficient. Therefore, it was explained that shadow leaves influenced on choice of sensitive bands when using vegetation index to evaluate chlorophyll density.

3 Discussion

The classification for targets in the image was achieved by normalized spectral index proposed in the paper. Compared with traditional classification method of remote sensing, separation in layers for different components was emphasized for targets in the field where target type was single, while the influence of many targets on classification result must be considered for traditional remote sensing classification. Secondly, the relevance with its biochemistry index was analyzed after spectral information of pure crops was collected; by comparing the result of mixed targets with that before purification, it was found the relevant coefficient and determination coefficient after purification were obviously higher than the mixed result, which provided key research concept for construction of small-scale quantitative model of crop biochemistry parameter.

Computer visualization technology is always an important means to judge crop′s life information. Although there are some advantages of quickly getting information and little disturbance from environment, etc, it cannot be extensively used to diagnose for crop nutrient, pest and disease damage, and it also is seriously restricted for it only contained a little information in blue, green, and red region; furthermore, only qualitative analysis was applied and the demand of current quantitative remote sensing in agriculture could not be satisfied. The imaging spectra has real-time im aging characteristic that spectra at

certain parts was collected according to variation part in the figure in order to achieve quantitative analysis for nutrient, pest and disease damage threat of single crop leaf or in group level.

Detection researches of crop spectra were frequently conducted using ASD. Data obtained by this spectrometer was composed by mixed spectra of different targets, the mixture of vegetation, soil, weeds and crop straw, etc. At present, most diagnosis models for nutrient, water, pest and disease damage threat set up by domestic and foreign researchers with spectra data were mostly influenced by background targets[20]. Although influence of background targets on spectra data was reduced by vegetation index built by some scholars or adopting differentiation spectral treatment methods, the influence of different illumination and background targets on model precision still existed[23]. The spectral information of research target can be purified by imaging classification in near-ground imaging spectra particularly the influence of soil background on mixed spectra was discussed and the influence of different illumination and shadow ratios on imaging spectra data was studied. It had extremely important significance in observation research of multiple angles.

4 Conclusions

The normal ized spectral index that was the classification method for imaging-based targets, was proposed based on normalized spectral reflectance. This method contained green, red and near-red spectral characteristics, different from traditional remote sensing imaging classification and digital imaging classification methods.

After spectral information of pure crop and target with soil background in the images were purified based on imaging classification, it was found great different between mixed spectra and pure crop spectra at near-infrared band; furthermore, reflectivity of pure crop was rapidly dropped soil background was masked and the drop was biggest at near-infrared band.

Normalized spectral classification index was applied in soybean spectra image that spectral information was collected for pure soybean vegetation, soil, sun leaves and shadow leaves and spectral influence for those components on crop chlorophyll density inversion was analyzed one by one; it was found that: shadow leaves influenced on choice for vegetation chlorophyll density sensitive band.

References:

[1] Rogan John, Jennifer Miller, Doug Stow, et al. Land-Cover change monitoring with classification trees using landsat tm and ancillary data [J]. ***Photogrammetric Engineering & Remote Sensing***, 2003, 69 (7): 793-804.

[2] Gong P, Pu R, Biging G S, et al. Estimation of forest leaf area index using vegetation indices derived from hyperion hyperspectral data[J]. ***IEEE Transactions on Geoscience and Remote Sensing***, 2003, 41(6): 1355-1362.

[3] Boggs G S. Assessment of SPOT 5 and QuickBird remotely sensed imagery for mapping tree cover in savannas [J]. ***International Journal of Applied Earth Observation and Geoinformation***, 2010, 12: 217-224.

[4] Zhang X, Feng X, Jiang H. Object-oriented method for urban vegetation mapping using IKONOS imagery [J]. ***International Journal of Remote Sensing***, 2010, 31(1): 177-196.

[5] Yang M, Zhao C, Zhao Y, et al. Research on a method to derive wheat canopy information from airborne imaging spectrometer data [J]. ***Scientia Agricultura Sinica***, 2002, 35 (6): 626-631.

[6] Kumara A S, Keerthi V, Manjunath A S, et al. Hyperspectral image classification by a variable interval spectral average and spectral curve matching combined algorithm [J]. ***International Journal of Applied Earth Observation and Geoinformation***, 2010, 12: 261-269.

[7] Martin D P, Rybicki E P. Microcomputer-based quantification of maize streak virus symptoms in Zea mays [J]. ***Phytopathology***, 1998, 88(5): 422-427.

[8] Lukina E V, Stone M L, Raun W R. Estimating vegetation coverage in wheat using digital images[J]. ***Journal of Plant Nutrition***, 1999, 22(2): 341-350.

[9] Ahmad I S, Reid J F, Paulsen M R, et al. Color classifier

for symptomatic soybean seeds using image processing [J]. ***Plant Disease***, 1999, 83(4): 320-327.

[10] Shi Y, Deng J, Chen L, et al. Leaf characteristics extraction of rice under potassium stress based on static scan and spectral segmentation technique [J]. ***Spectroscopy and Spectral Analysis***, 2010, 30(1): 214-219.

[11] Scharf P C, Lory J A. Calibrating corn color from aerial photographs to predict sidedress N need [J]. ***Agronomy Journal***, 2002, 94: 397-404.

[12] Jia L, Chen X, Zhang F, et al. To detect nitrogen status of inter wheat by using color digital camera [J]. ***J Plant Nutrition***, 2004, 27(3): 441-450.

[13] Tong Q, Xue Y, Wang J, et al. Development and application of the field imaging spectrometer system [J]. ***Journal of Remote Sensing***, 2010, 14(3): 409-422.

[14] Zhang D Y, Liu L Y, Huang W J, et al. Inversion and evaluation of crop chlorophyll density based on analyzing image and spectrum [J]. ***Infrared and Laser Engineering***, 2013, 42(7): 1871-1181.

[15] Christian Nansen, Tulio Macedo, Rand Swanson, et al. Use of spatial structure analysis of hyperspectral data cubes for detection of insect-induced stress in wheat plants [J]. ***International Journal of Remote Sensing***, 2009, 30 (10): 2447-2464.

[16] Chai A, Liao N, Tian L. Identification of cucumber disease using hyperspectral imaging and discriminate analysis [J]. ***Spectroscopy and Spectral Analysis***, 2010, 30(5): 1357-1361.

[17] Inoue Y, Penuelas J. An AOTF-based hyperspectral imaging system for field use in ecophysiological and agricultural applications [J]. ***International Journal of Remote Sensing***, 2001, 22(18): 3883-3888.

[18] Tan H, Li S, Wang K, et al. Monitoring canopy chlorophyll density in seedlings of winter wheat using imaging spectrometer [J]. ***Acta Agronomica Sinica***, 2008, 34 (10): 1812-1817.

[19] Zhang L, Huang C, Wu T, et al. Laboratory calibration of a field imaging spectrometer system [J]. ***Sensors***, 2011, 11: 2408-2425.

[20] Huang W. Remote sensing monitoring of crops diseases mechanism and application [J]. ***China's Agricultural Science and Technology Press***, 2009: 18-24.

[21] Wang J, Zhao C, Huang W. Basis and Application of Quantitative Remote Sensing in Agriculture [M]. Beijing: Science Press, 2008: 5-11.

[22] Yu B I, Michael Ostland, Peng Gong. Penalized discriminant analysis of in situ hperspectral data for conifer species recognition [J]. ***IEEE Transactions on Geosciences and Remote Sensing***, 1999, 5(37): 2569-2576.

[23] Pu R. Broadleaf species recognition with in situ hyperspectral data[J]. ***International Journal of Remote Sensing***, 2009, 30: 2759-2779.

[24] Zhang D Y, Liang D, Zhao J L, et al. Bidirectional reflectance characteristics of soybean canopy using multi-angle hyperspectral imaging [J]. ***Infrared and Laser Engineering***, 2013, 42(3): 787-797.

[25] Haboudane D, Tremblay N, Miller J R, et al. Remote estimation of crop chlorophyll content using spectral indices derived from hyperspecral data [J]. ***IEEE Transaction on Geoscience and Remote sensing***, 2008, 46: 423-427.

[26] Gitelson A A, Kaufman Y, Merzlyak M. Use of a green channel in remote sensing of global vegetation from EOS-MODIS [J]. ***Remote Sensing of Environment***, 1996, 58(3): 289-298.

[27] Hansen P M, Schjoerring J K. Reflectance measurement of canopy biomass and nitrogen status in wheat crops using normalized difference vegetation indices and partial least squares regression [J]. ***Remote Sensing of Environment***, 2003, 86: 542-553.

[28] Roshanak Darvishzadeh, Andrew Skidmore, Artin Chlerf, et al. Inversion of a radiative transfer model for estimating vegetation LAI and chlorophyll in heterogeneous grassland[J]. ***Remote Sensing of Environment***, 2008, 112: 2592-2604.